Two-Dimensional Turbulent Flow and Heat Transfer in Tall Glazing Cavities

Joseph P. Power, Ph.D.
Student Member ASHRAE

Dragan Curcija, Ph.D.
Member ASHRAE

William P. Goss, Ph.D.
Member ASHRAE

ABSTRACT

There have been a number of analytical studies made for predicting heat transfer in high aspect ratio (cavity height to width) glazing cavities, but very few studies have been performed for situations where the flow in the cavity is turbulent. For high aspect ratio (A) glazing cavities, buoyancy-driven turbulent flow will occur at moderate Rayleigh Numbers (Ra_L). The presence of turbulence in the glazing cavity can have a significant effect on the cavity flow pattern and heat transfer rate.

In the present study, two-dimensional laminar and turbulent natural convection heat transfer of air in high aspect ratio rectangular cavities was analyzed using a finite-element turbulent computational fluid dynamic solution method. The numerical analysis includes the effects of laminar and turbulent natural convection and radiant heat transfer within the cavity. The fenestration systems studied were a prototype casement window and an argon-filled double-glazing unit. Comparisons of the laminar and turbulent heat transfer calculation results are made with the experimental results. The laminar and turbulent heat transfer model-calculated results showed good agreement with the experimental results for cavity flows in the transitional region between the laminar and turbulent flow regimes.

INTRODUCTION

The classic problem of natural convection heat transfer in a cavity has been well studied for many years. Numerous experimental studies have been done for laminar cavity flows. More recently, numerical calculations have been successful in predicting laminar flow and heat transfer in cavities. As experimental and numerical procedures have improved, more realistic situations have been successfully calculated numerically. The improvements include full natural convection models with radiation effects in two dimensions by Wright (1990) and two- and three-dimensions by Curcija (1992). The present study continues to the next level of complexity by numerically calculating the heat transfer in a fenestration system with the presence of turbulence in the glazing cavity.

Numerous numerical methods have been proposed for the computer simulation of turbulent flow (e.g., Ince [1984], Betts and Dafa'Alla [1986]). The description of the turbulent effects has progressed into the now common two-equation turbulence models. Recently, a low Reynolds number model was proposed by Wilcox (1993) that is well suited for the low-speed conditions in buoyancy-driven cavity flows.

The motion of air in a double-glazed fenestration cavity will become turbulent when certain criteria are met. The controlling parameters are the physical dimensions of the cavity (i.e., the cavity width and height), the properties of the fluid, and the temperature difference across the cavity. One of the characteristics of turbulent flow is larger scale (than molecular) mixing, which results in increased rates of heat transfer. This increase in heat transfer is undesirable for a glazing cavity in a fenestration product that is designed to retard the flow of heat while allowing a view to the outside.

This paper presents numerical results of the thermal behavior of a prototype casement window (Fisher [1994], designated as PFM02) and an argon-filled double-glazing unit (Van Dijk [1997], designated as IEA) using a finite-element solution technique. The finite element mesh was developed and the calculations performed using a general purpose finite-element heat transfer and fluid flow program (FDI 1996). The results from the calculations are compared with experimental data obtained from a calibrated hot box. The comparisons include U-factors and temperature distributions. Tests were performed according to ASTM C1199-97 (ASTM 1997) for winter nighttime conditions. The U-factors were calculated

Joseph P. Power is a development engineer at Engineering Solutions International, Ltd., Dublin, Ireland. **Dragan Curcija** is president of Carli, Inc., Amherst, Mass. **William P. Goss** is a professor in the Department of Mechanical and Industrial Engineering, University of Massachusetts, Amherst.

according to *ANSI/ASHRAE Standard 142P* (ASHRAE 1996).

Figure 1 is a drawing indicating components and boundary conditions of the PFM02 window. Figure 2 contains a dimensioned drawing of the bottom portion of the window. The overall dimensions of the PFM02 window are 91.4 cm (36 in.) high by 61cm (24 in.) wide with a cavity width of 16.5 mm (0.65 in.) and an aspect ratio (cavity height divided by the width) of $A = 50.19$. Figure 3 is a drawing indicating components and boundary conditions for the bottom portion of the IEA glazing unit. The overall dimensions of the IEA glazing unit are 120 cm (47.3 in.) by 120 cm (47.3 in.) with a cavity width of 16 mm and an aspect ratio of $A = 74$. Table 1 gives the material properties used for the PFM02 window and the IEA glazing unit.

Natural convection heat transfer can be modeled mathematically by a set of governing equations derived from the conservation of mass, Newton's second law, and the first law of thermodynamics. Application of these basic laws to an infinitesimal control volume along with appropriate boundary conditions gives a mathematical model of the natural convection heat transfer that occurs in fenestration system glazing cavities. The resulting system of partial differential equations is referred to as the Navier-Stokes equations. In order to obtain a numerical solution for turbulent flow, Reynolds decomposition is applied to these equations, which decomposes the variables into instantaneous (fluctuating) and mean (time averaged) components. The Reynolds averaged, approximate

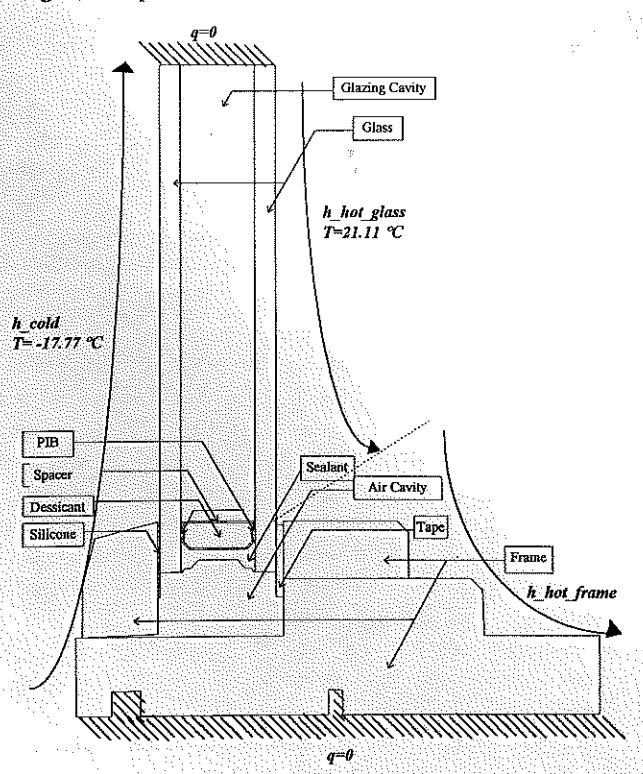

Figure 1 *PFM02 window boundary conditions and material locations.*

Navier-Stokes equations are solved along with additional turbulence governing equations. The turbulence closure equations are necessary to account for the additional turbulent flow variables. Details of the derivation of the Navier-Stokes and the turbulence governing closure equations can be found in Currie (1993) and Wilcox (1993). The resulting system of partial differential equations is given below in Cartesian tensor notation.

Conservation of mass:

$$\partial_i U_i = 0 \tag{1}$$

Newton's second law (conservation of momentum):

$$\rho\partial_0(U_i) + \rho U_j\partial_j(U_i) = \partial_i P + (\mu + \mu_T)\partial_i(\partial_j U_i + \partial_i U_j) + \rho\beta g_i(T - T_o) \tag{2}$$

First law of thermodynamics (energy equation):

$$\rho(\partial_0 T + u_i\partial_i T) = \left(\frac{\mu}{Pr} + \frac{\mu_T}{\sigma_T}\right)\partial_i\partial_i T \tag{3}$$

Turbulence kinetic energy:

$$\begin{aligned}\rho\partial_0 k + \rho U_j\partial_j k &= \mu_T(\partial_j U_i + \partial_i U_j) + \\ \partial_j U_i - pk\omega + \partial_j\left[\left(\mu + \frac{\mu_T}{\sigma_k}\right)\partial_j k\right] &+ \beta\frac{\mu_T}{\sigma_T}\partial_i T g_i\end{aligned} \tag{4}$$

Specific dissipation rate of turbulence kinetic energy:

$$\begin{aligned}\rho\partial_0\omega + \rho U_j\partial_j\omega &= \alpha'\frac{\omega}{k}\mu_T(\partial_j U_i + \partial_i U_j)\partial_j U_i - \beta'\rho\omega^2 + \partial_j \\ &\left[\left(\mu + \frac{\mu_T}{\sigma_\omega}\right)\partial_j\omega\right] + \alpha'(1 - c_3)\beta\frac{\mu_T}{\sigma_T}\partial_i T g_i\frac{\omega}{k}\end{aligned} \tag{5}$$

Auxiliary relations and closure coefficients:

$$\varepsilon = k\omega \quad u_T = k^{\frac{1}{2}} \quad l_T = \frac{k^{1/2}}{\omega} \quad \mu_T = \frac{c_\mu\rho k}{\omega} \tag{6}$$

$$\sigma_k = 2 \quad \sigma_\omega = 2 \quad \alpha' = \frac{5}{9} \quad \beta' = \frac{3}{40} \quad c_\mu = \frac{9}{100} \quad \sigma_T = \frac{9}{10} \quad c_3 = \frac{4}{5} \tag{7}$$

When the heat transfer for an entire fenestration system is numerically calculated, radiation effects in the cavity need to be accounted for. The radiant heat transfer in a real glazing cavity with top and bottom surfaces and variable temperatures along the cavity surfaces is complex. It involves the use of the surface element radiosities and the view (shape, configuration) factors between each pair of elements that make up the cavity surfaces. This is incorporated into the finite element analysis along with the conductive and convective heat transfer analysis. A detailed description of radiant heat transfer analysis and view (shape, configuration) factors is given in

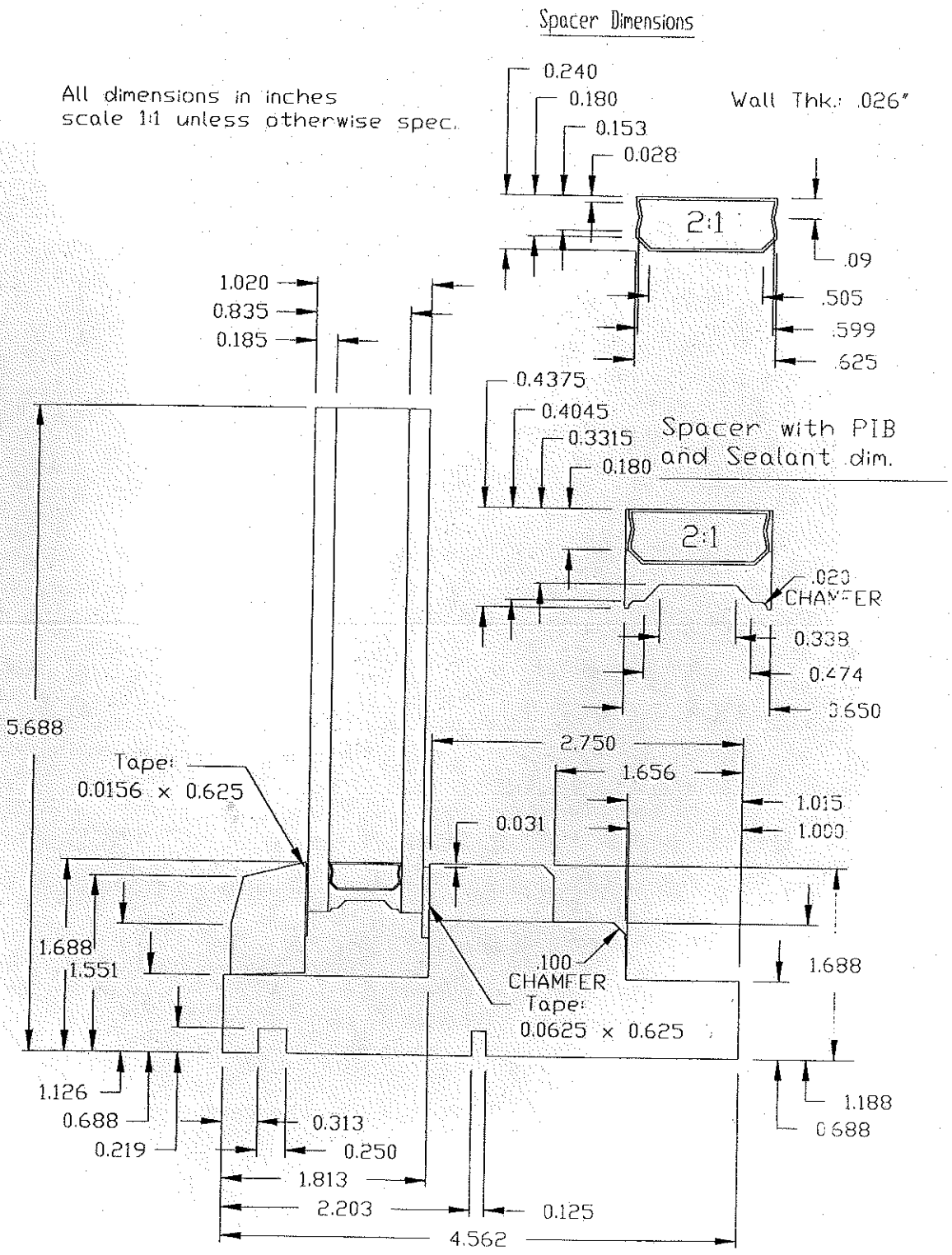

Figure 2 *PFM02 window dimensioned drawing.*

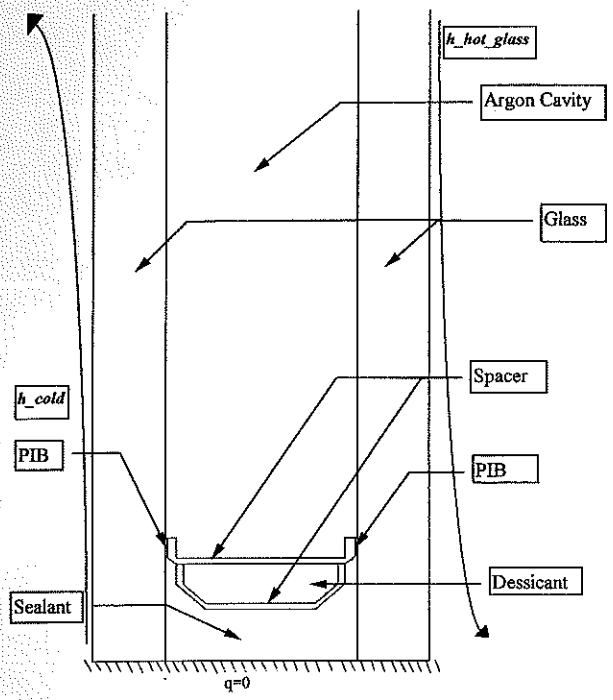

Figure 3 *IEA glazing boundary conditions and material locations.*

ASHRAE Fundamentals (ASHRAE 1997), Siegel and Howell (1992), and Power (1999).

NUMERICAL CALCULATION TECHNIQUE

The numerical solution of the governing equations is performed using the finite element method. The specific method used was the Galerkin method of weighted residuals. Essentially, the finite element method transforms an unsolvable set of differential equations into an approximate solvable set of nonlinear algebraic equations. The finite element discretization of the governing equations for laminar flow are given in Curcija (1992) and the discretization of the governing equations for turbulent flow are given in FDI (1996) and Power (1999). The property values of the cavity gases were calculated using cavity wall temperature data from a one-dimensional conduction model, Window 4.1 (LBL 1994). The average of these temperatures was used with the equations for air in NBS (1955) and for argon in ASHRAE Standard 142P (ASHRAE 1996) to determine the required fluid property values. The property values used in this study are given in Table 2.

The boundary conditions for the PFM02 window and the IEA glazing unit calculations are: adiabatic conditions at the top and bottom of the model; constant overall (radiation and conduction) surface heat transfer coefficients on the indoor glass and frame (different coefficients for indoor glass and frame surfaces) and the entire outdoor surfaces; no-slip velocity condition on all surfaces in contact with a gas (air or argon);

TABLE 1
Material Properties of Components in Window PFM02 and IEA Glazing

		PFM02 (Air Cavity)	IEA (Argon Cavity)
Part	**Name**	**Conductivity W/(m·°K)**	**Conductivity W/(m·°K)**
Glass panes	Glass	0.9	0.8
IGU cavity gas	Cavity	0.02386	0.01626
Spacer(Alum - SS)	Spacer	159.98	100
Desiccant beads	Desiccant	0.03	0.030
PIB sealant	Pib	0.24	0.20
Urethane sealant	Sealant	0.31	0.19
Silicon sealant	Silicon	0.36	NA
Poly-foam tape	Tape	0.24	NA
Wood frame	Frame	0.14	NA
Frame cavity	Air cavity	0.095	NA

NOTE: NA = Not Applicable.
Aluminum spacer for the PFM02 window.
Stainless steel spacer for the IEA glazing unit.

and "gray body" radiant heat transfer between all elements on the surfaces of the glazing cavity. The boundary condition data are given in Table 3.

A nine-node quadrilateral isoparametric element was used for all of the numerical calculations and was meshed using FDI (1996). The cavity density used for the PFM02 window and IEA glazing unit are 22 by 160 elements and 22 by 242 elements, respectively.

TRANSITION TO TURBULENCE

Previously published work by Batchelor (1954) focused on the transition from the conduction regime to the boundary layer flow regime and transition from laminar to turbulent regime. Yin et al.(1978) contained measurement data that fluctuated at sufficiently high Ra, and Wright (1990) interpreted this as an indication of the transition to turbulence. The correlations from these publications are given by Equations 8, 9, and 10.

Bathchleor (1954) Conduction to Boundary Layer

$$1<A\ 100:\ Ra = 500(A) \tag{8}$$

Batchelor (1954) Lam to Turbulent for

$$1<A<42:\ Ra = 10^9 \cdot (A)^{-3} \tag{9}$$

$$A>42:\ Ra = 13700$$

Wright (1990) Lam to Turbulent for

$$1<A<100:\ Ra = 2.86 \cdot 10^9 (A)^{-3} \tag{10}$$

TABLE 2
Property Values for PFM02 Window and IEA Glazing

Parameter	PFM02-Air	IEA-Argon	Units
Temperatures Obtained from Window 4.1 LBL(1994)			
Inside (hot) glass temperature	284.85	285.25	K
Outside (cold) glass temperature	258.15	258.15	K
Mean cavity temperature	271.50	271.70	K
Delta T	26.70	27.10	K
Thermal Physical Properties			
Dynamic viscosity	1.7037E-05	2.1115E-05	kg/(m·s)
Conductivity	0.02399	0.01626	W/(m·K)
Specific heat	1005.7	521.95	J/(kg·K)
Coefficient of volumetric expansion	0.003683	0.003680	1/K
Universal gas constant	8314	8314	(N-m)/(kmol-K)
Molecular weight	28.97	39.95	kg/kmol
Pressure (atmospheric)	101300	101300	N/m^2
Density	1.3001	1.7915	kg/m^2
Gravity	9.807	9.807	m/s^2
Characteristic length (cavity width)	0.01651	0.016	m
Thermal diffusivity	1.8344E-05	1.7385E-05	m^2/s
Non Dimensional Numbers			
Rayleigh Number	18,055	19,552	
Prandtl Number	0.7144	0.6780	
Grashof Number	25,274	28,839	
Stefan Boltzman constant	5.6705E-08	5.6705E-08	$W/(m^2 \cdot K^4)$

An aspect ratio vs. Rayleigh number plot containing the correlations from Batchelor (1954) and Wright (1990) (transition laminar to turbulent flow) and the location of the PFM02 window and IEA glazing unit are presented in Figure 4. The location of PFM02 window is in between the correlation lines by Wright (1990) and Batchelor (1954) for the transition to turbulence. The IEA glazing unit is to the right (turbulent flow regime) of both correlations. It should be noted that based on the original Batchelor (1954) laminar to turbulent flow correlation both the PFM02 window and the IEA glazing unit were well within the turbulent flow regime. More recent work by Power (1999) indicated that both of these fenestration products were in the transition region as the flow goes from laminar to turbulent flow. Figure 4 has the Batchelor sloped line changing to a vertical line at an aspect ratio of approximately 40 to indicate this preliminary finding.

To determine the effects of turbulence in the current numerical calculations, the average Nusselt number for calculations of transient laminar cavity flow was plotted vs. time. The implicit transient solution iterates each time step, and the converged numerical solution for each time step is used for comparisons to turbulent flow. This will show if the transient solution is changing with time. The laminar data are then compared with the turbulent flow solution. The PFM02 window had a steady laminar flow, which had a slightly lower rate of cavity heat transfer than that for turbulent flow. The IEA glazing unit has a non-steady laminar solution with the fluctuations in the Nusselt number approximately one percent of the overall average Nusselt number.

RESULTS

Several types of numerical calculations were preformed for both the PFM02 window and IEA glazing unit. These include the idealized one-dimensional conduction using

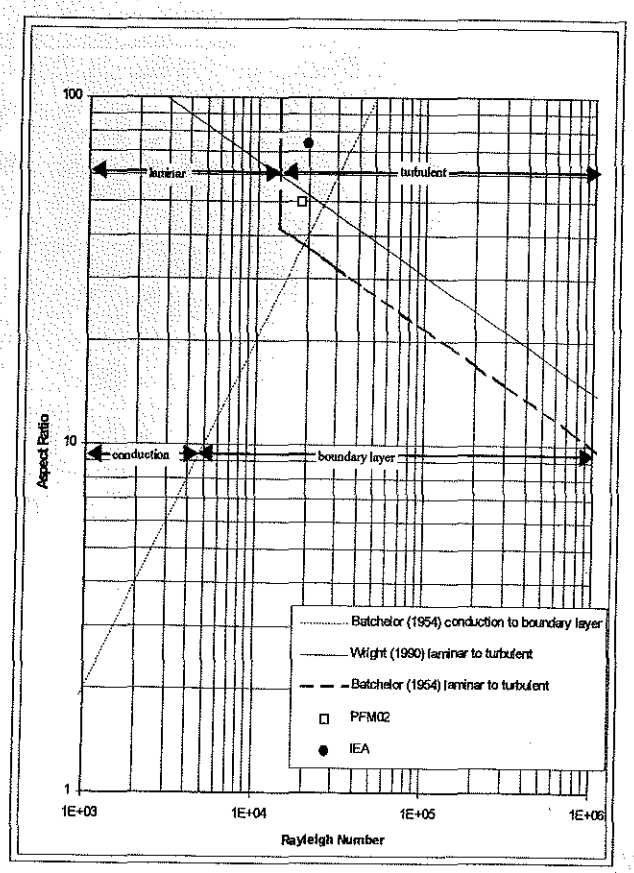

Figure 4 *Aspect ratio vs. Rayleigh number transition to turbulent flow.*

TABLE 3
Boundary Conditions for PFM02 Window and IEA Glazing Unit

		PFM02	IEA	
Location	**Name**	**Value**	**Value**	**Reference Temperature**
Indoor Glass	h_hot_glass	$h_{i\,glass}$ =7.9W/m^2·°C	$h_{i\,glass}$ =7.9 W/m^2·° C	21.11°C
Indoor Frame	h_hot_frame	$h_{i\,frame}$ =7.6W/m^2·°C		21.11°C
Outdoor	h_cold	h_o =28.7W/m2·°C	h_o =28.7 W/m^2·°C	−17.77°C
Bottom of Frame	Bottom	q=0 W/m^2 (ZHF)	q=0 W/m^2 (ZHF)	NA
Top of Frame	Top	q=0 W/m^2 (ZHF)	q=0 W/m^2 (ZHF)	NA
Emissivity of Glass	Cavity cold	$\tilde{\varepsilon}$ = 0.84	$\tilde{\varepsilon}$ = 0.84	NA
	Cavity hot	$\tilde{\varepsilon}$ = 0.09	$\tilde{\varepsilon}$ = 0.18	NA

NOTE: NA - reference temperature not required for ZHF boundary condition.

WINDOW 4.1 (LBL 1994); two-dimensional conduction by THERM (LBL 1996) where an equivalent overall thermal conductivity is used in the cavity; and two-dimensional frame conduction with either laminar flow or turbulent flow in the glazing cavity using FDI (1996).

PFM02 Results

Temperature values for the PFM02 window for all three numerical calculations (conduction only, laminar flow, and turbulent flow) are shown in Figure 5. Also included in Figure 5 are the measurement data (measurement data shown as points with ±1 °C error bars) and the WINDOW4.1 center-of-glass data point. The distance given in Figure 5 is measured from the bottom of the PFM02 window. The temperatures given are for the indoor side, which is of primary interest due to potential condensation effects. In the top and bottom frame regions, all three numerical calculations give the same result since there are no internal flow effects present, so all three are modeling conduction only through the frame. The laminar and turbulent flow results show excellent agreement in the center and the edge-of-glass regions (length values between 0.8 and 0.9) of the window. The wavy variations in the laminar flow solution show the existence of multicellular flow in the center region. This agrees with Wright (1990), who showed the existence of a multicellular flow pattern in a glazing cavity for a

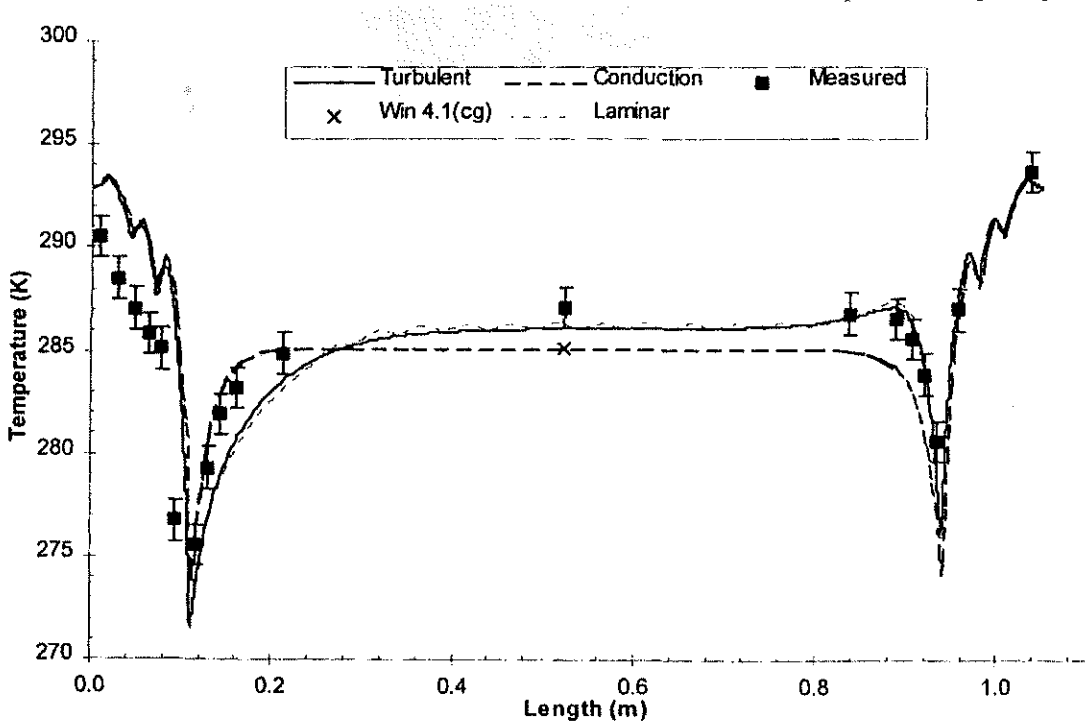

Figure 5 *PFM02 window—indoor temperature vs. distance.*

TABLE 4
PFM02 Center-of-Glass Temperature Difference Using the Experimental Data as the BASE

Program	Hot Side		Cold Side	
	T_{cg} ° K	Percent Difference Base = 286.27 °K	T_{cg} ° K	Percent Difference Base = 256.34 °K
FIDAP Turbulent	286.10	−0.06%	257.61	0.50%
FIDAP Laminar	286.23	−0.01%	257.60	0.49%
FIDAP Cond	285.17	−0.38%	257.87	0.60%
Therm	284.99	−0.45%	257.92	0.62%
Experimental	286.27	–	256.34	–

sufficiently high Rayleigh number. The laminar and turbulent flow numerical calculations underpredicted the measured temperatures for the bottom edge-of-glass region (length between 0.1 and 0.2). All three numerical results overpredict the experimental results for the bottom frame (length between 0 and 0.1). This discrepancy between the measured and calculated results in the bottom regions may be due to the boundary condition used. The indoor boundary conditions may not accurately represent the actual irregular flow patterns over the frame due to stagnation and separation regions, as the inside surface natural convection flow attempts to follow the contours of the frame profile. This can cause local variations in the local surface heat transfer coefficients and surface temperatures. The indoor radiant heat transfer coefficient is based on only seeing an indoor baffle at constant temperature. Therefore, the radiant heat transfer between the glass and the frame profile is also not accounted for and can cause some of the temperature discrepancies between the numerical results and the measured data. The indoor radiant heat transfer coefficient is combined with an indoor convective heat transfer coefficient, which give a constant overall glass surface and frame indoor surface heat transfer coefficients. These combined overall heat transfer coefficients are used as boundary conditions in the laminar and turbulent flow numerical calculations. This indicates the need to go to variable overall surface heat transfer coefficients based on the actual window geometry for condensation resistance purposes. This would include a variable convective heat transfer coefficient due to frame profile changes and element to element radiant heat transfer to include frame glazing radiation exchange.

The center-of-glass region of the laminar solution has a wavelike pattern, indicating the presence of cells in the cavity. There are no such cells for the turbulent temperature profile. The turbulence equations appear to have a dampening effect on the flow pattern where the dissipative nature of the turbulent flow may have disrupted the cell pattern in the center-of-glass region. Due to the wavelike temperature pattern, an average temperature around the center-of-glass area is used for comparison of the laminar solutions to the other numerical and experimental results.

Table 4 contains center-of-glass temperature values for the experimental data and numerical calculations for both the indoor and outdoor glass surfaces. Table 4 also contains percent difference values of the calculated temperatures where the measurement data are used as the base. The center-of-glass temperature for the laminar and turbulent solutions in Table 4 are both within 0.1% of the experimental data.

U-factors were also calculated for both the experimental and numerical results. Table 5 contains overall U-factors for the measured and numerical results and percent difference values, which use the measurement data as the base. Both the turbulent and laminar results were within 1.5% of the measured data. The detailed output from the laminar and turbulent flow models indicated that the flow was in the initial stages of turbulent flow in the glazing cavity, which is why the two flow models are in good agreement (Power 1999). It should be noted that while ASTM C1199-97 (ASTM 1997) does not have an experimental uncertainty procedure specified yet, preliminary estimates of the experimental uncertainty of the calibrated hot box indicate an uncertainty of 5% to 8% in the overall U-factor for nonhomogeneous test specimens such as fenestration products. Therefore, achieving a less than 1.5% difference between the calculated and the experimental U-factors is fortuitous.

TABLE 5
PFM02 U-Factor Difference Using the Experimental Data as the BASE

Program	U-Overall W/(m^2· °K)	Percent Difference to Base Base = 1.917 W/(m^2· °K)
FIDAP Turbulent	1.906	−0.56%
FIDAP Laminar	1.896	−1.11%
FIDAP Cond	1.999	4.26%
Therm	2.039	6.39%
Experimental	1.917	-

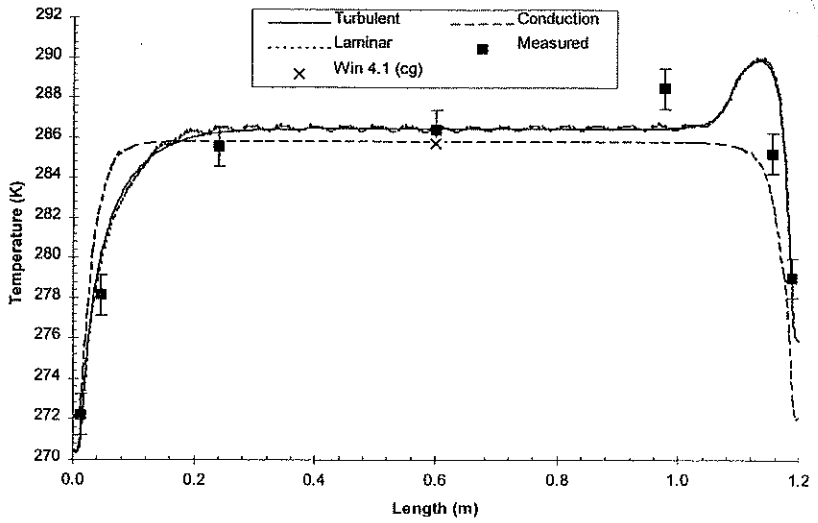

Figure 6 *IEA glazing—indoor temperature vs. distance.*

IEA Results

Temperature values for the IEA glazing unit for all four numerical calculations plus the WINDOW 4.1 center-of-glass single data point, along with experimental temperature data, are shown in Figures 6 and 7. Figure 6 contains the temperature profiles for the indoor (hot) surface, and Figure 7 contains the temperature profiles for the outdoor (cold) surface. The distance given in Figures 6 and 7 is measured from the bottom of the IEA glazing unit.

Due to the fluctuating nature of the laminar solution of the IEA glazing unit, temperature and heat flow data have been averaged over the last 500 (samples at 25 time step intervals) time steps. The cells were changing location in the glazing cavity, and averaging the temperature for each converged time step had a smoothing effect (a sine wave pattern emerges as if the cells were not moving) on the IEA data. A plot of temperature vs. distance for a single time step had an irregular (non-sine-wave) profile. These irregularities and the random nature of the laminar solution would again appear to indicate the presence of turbulence in the cavity (Power 1999). Due to the wavelike temperature pattern, an average temperature around the center-of-glass area is used for comparison of the laminar solutions to the other numerical and measured results.

Figure 6 and Figure 7 show good agreement between the time-averaged laminar and turbulent flow results with the measured data. This may be in part due to the flat surface of the IEA glazing unit, which lends itself to the early development of a uniform boundary layer along the glazing surface

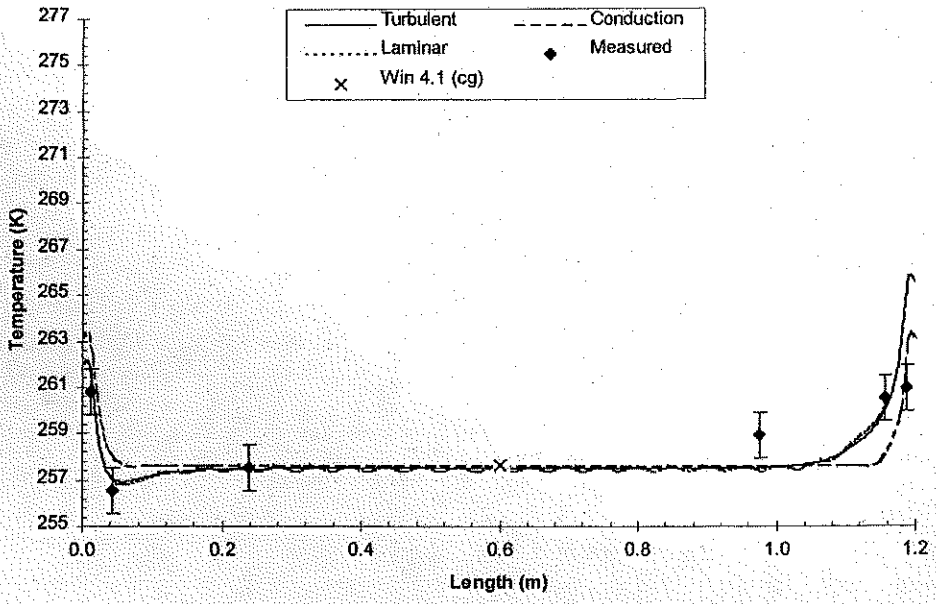

Figure 7 *IEA glazing—outdoor temperature, cold side vs. distance.*

TABLE 6
IEA Center-of-Glass Temperature Difference Using the Experimental Data as the BASE

Program	Hot Side		Cold Side
	T_{cg} °K	Percent Difference Base = 286.4 °K	T_{cg} °K
FIDAP Turbulent	286.46	0.02%	257.52
FIDAP Laminar	286.53	0.05%	257.54
FIDAP Cond	285.85	−0.19%	257.68
Therm	285.85	−0.19%	257.69
Experimental	286.40	—	NA

NOTE: NA - experimental center-of-glass temperature data not available.

(the frame profile geometry problems associated with PFM02 are not seen here). For both the hot and cold sides, there is some discrepancy for the thermocouple reading near the interface between the center and edge of glass (location of approximately 0.9 m from the bottom of the glazing).

The center-of-glass region of the laminar solution has a wavelike pattern, indicating the presence of cells in the cavity. There are no such cells for the turbulent temperature profile. As previously stated for the PFM02 window, the turbulence equations may have a dampening effect on the flow pattern, or the cells may not exist.

Table 6 contains center-of-glass temperature values for the measurement data and numerical calculations and percent difference values that use the measurement data as the base. Only the indoor (hot side) center-of -glass data are available from the experimental results. The center-of-glass temperature for the both the laminar and turbulent solutions in Table 6 are within 0.5%of the experimental data.

U-factors were also calculated for both the experimental and numerical results. Table 7 contains overall U-factors for the measurement and numerical results and percent difference values that use the measurement data as the base. The turbulent and laminar solutions were within 1.5% when compared to the measured U-factor. Again, the output from the turbulent flow model indicated the onset of turbulent flow in the glazing cavity (Power 1999).

TABLE 7
IEA U-Factor Difference Using the Experimental Data as the BASE

Program	U-Overall W/(m^2· K)	Percent Difference to Base Base = 1.836 W/(m^2· K)
FIDAP Turbulent	1.821	−0.56%
FIDAP Laminar	1.813	−1.26%
FIDAP Cond	1.861	1.33%
Therm	1.863	1.46%
Experimental	1.836	—

CONCLUSIONS AND RECOMMENDATIONS

The turbulent flow numerical calculations for both fenestration systems compared quite well with the measured data. There were indications of the presence (or at least the beginnings) of turbulence for the PFM02 window, while there were stronger indicators for the IEA glazing unit. The turbulent flow model can also be used to predict the thermal performance of fenestration products, such as commercial skylights and coupled windows with wider gap glazing cavities, where turbulent flow is predominant and laminar flow models are inadequate.

Future work on the turbulent flow cavity heat transfer model described in this paper should concentrate on extending the laminar flow correlations developed by Zhao et al. (1998) and extending the range of Raleigh numbers and aspect ratios to include fully turbulent flow in glazing cavities. This work should also develop correlations for predicting the transition region from laminar to turbulent flow. The surface temperature discrepancies in both the laminar and turbulent flow models, when compared with experimental surface temperature data, should be addressed by applying more realistic, varying, overall convective heat transfer coefficient boundary conditions in both models.

NOMENCLATURE

Symbols

A = aspect ratio
C_3 = closure coefficient
C_p = specific heat (energy/(mass×degree)
∂_o = $\partial()/\partial t$
∂i = $\partial()/\partial x_i$
g = gravitational acceleration (length/time^2)
H = height (cavity [length])

h = convective heat transfer coefficient (energy/(time×length^2×degree))

h_i = convective heat transfer coefficient (indoor) (energy/(time×length^2×degree))

h_o = convective heat transfer coefficient (outdoor) (energy/(time×length^2×degree))

k = specific turbulence kinetic energy (length^2/time^2)

$\hat{n}$ = unit normal vector

P = pressure (force/length^2 = mass/(length×time^2))

q = heat flux (energy/length^2 = mass/time^2)

Q = total heat flow (energy = (mass×length^2)/time^2)

T = temperature (degree)

u = x component of velocity (length/time)

u_T = turbulent characteristic velocity (length/time)

U = x component of mean velocity (length/time)

U = heat transfer coefficient (energy/(time×length^2×degree)

U_∞ = characteristic velocity (length/time)

v = specific volume (length^3/mass)

v = y component of velocity (length/time)

V = y component of mean velocity (length/time)

x, y = Cartesian coordinate directions

NOTE: Degree is a degree of temperature, energy = (mass×length^2)/time^2

Greek Symbols

α = coefficient of thermal diffusion (length^2/time)

α' = closure coefficient

β = coefficient of thermal expansion (1/degree)

β' = closure coefficient

c_μ = closure coefficient

$\tilde{\varepsilon}$ = surface emissivity

ε = specific dissipation rate of turbulence kinetic energy (length^2/time^3)

ℓ = characteristic length (length)

ℓ_T = turbulence characteristic length (length)

λ = thermal conductivity (energy/(time×length×degree))

μ = dynamic viscosity (mass/(length×time)

μ_T = eddy viscosity (mass/(length×time))

r = density (mass/ length^3)

σ = Stefan-Boltzmann constant (energy/(time×length^2×degree^4))

σ_ω = closure coefficient

σ_k = closure coefficient

ν = kinematic viscosity (length^2/time)

ν_T = kinematic eddy viscosity (length^2/time)

ω = specific dissipation rate of turbulence kinetic energy (1/time)

Dimensionless Groups

Rayleigh Number: $Ra_l = \frac{\rho\beta\Delta T l^3 g}{\alpha\mu}$

Prandtl Number: $Pr = \frac{\mu\rho}{\alpha} = \frac{C_p\mu}{\lambda}$

where $\alpha = \frac{\lambda}{C_p\rho}$

Grashof Number: $Gr = \frac{Ra}{Pr}$

Nusselt number: $Nu = \frac{ql}{\lambda}$(for cavity wall)

Reynolds number: $Re_x = \frac{\rho Ux}{\mu}$(for cavity wall)

ACKNOWLEDGMENTS

The authors wish to thank Marvin Windows and Doors and Mr. Steven Fisher for their assistance in providing test windows for use in this research. The authors would like to acknowledge the financial support of the Office of Building Systems of the United States Department of Energy under financial assistance award number DE-FG36-94CH10604. The authors would also like to acknowledge a supercomputer grant from the Energy Research Scientific Computing Center, which is supported by the Office of Energy Research of the United States Department of Energy. Without the above support, this research would not have been possible. Any opinions, findings, and conclusions or recommendations expressed in this paper are those of the authors and do not reflect the views of the above granting agencies.

REFERENCES

ASHRAE. 1997. *1997 ASHRAE Handbook—Fundamentals.* Atlanta: American Society of Heating, Refrigerating and Air-Conditioning Engineers, Inc.

ASHRAE. 1996. *ANSI/ASHRAE Standard 142P, Standard method for determining and expressing the heat transfer and total optical properties of fenestration products.* Atlanta: American Society of Heating, Refrigerating and Air-Conditioning Engineers, Inc.

ASTM. 1997. ASTM C1199-97, Standard test method for measuring the steady state thermal resistance of fenestration systems using hot box methods. *1998 Annual Book of ASTM Standards.* Philadelphia: American Society for Testing and Materiasl.

Batchelor, G.K. 1954. Heat transfer by free convection across a closed cavity between vertical boundaries at different temperatures. *Quarterly of Applied Mathematics,* 12: 209-223.

Betts, P.L., and A.A. Dafa'Alla. 1986. Turbulent buoyant air flow in a tall rectangular cavity, Significant questions in

buoyancy affected enclosure or cavity flows. ASME Annual Meeting, Boston, 1983, Collection of Papers.

Curcija, D. 1992. Three-dimensional finite element model of overall, night time heat transfer through fenestration systems. Ph.D. thesis, Department of Mechanical Engineering, University of Massachusetts, Amherst.

Currie, I.G. 1993. *Fundamentals mechanics of fluids*. McGraw-Hill, Inc.

FDI. 1996. *FIDAP 7.0, User's and reference manual.* Fluid Dynamics Analysis Package, Revision 7.0, Fluid Dynamics International.

Fisher, S. 1994. Private communications, Marvin Windows and Doors, Warroad, Minn.

Ince, N.Z. 1984. Experimental and numerical study of natural convection in tall cavities. Ph.D. thesis, Department of Mechanical Engineering, University of Manchester Institute of Science and Technology.

LBL. 1996. *THERM 1.0, A PC program for analyzing two-dimensional heat transfer through building products*. Program description. Windows and Daylighting Group, Lawrence Berkeley Laboratory, Berkeley, Calif.

LBL. 1994. *WINDOW 4.1, A PC program for analyzing window thermal performance—Program description and tutorial.* Windows and Daylighting Group,.Lawrence Berkeley Laboratory, Berkeley, Calif.

NBS. 1955. Tables of thermal properties of gasses. National Bureau of Standards Circular 564. U.S. Government Printing Office, November.

Power, J.P. 1999. Finite element model of turbulent heat transfer in fenestration system cavities. Ph.D. thesis, Department of Mechanical Engineering, University of Massachusetts, Amherst.

Siegel, R., and J.R. Howell. 1992. *Thermal radiation heat transfer.* Hemisphere Publishing Corp.

Van Dijk, D. 1997. Extract from Draft TNO Report, B14 Project IEA Task 19, 3/3/97.

Wilcox, D.C. 1993. *Turbulence modeling for CFD*. Griffin Printing.

Wright, J.L. 1990. The measurement and computer simulation of heat transfer in glazing systems. Ph.D. thesis, Department of Mechanical Engineering, University of Waterloo, Waterloo, Ontario.

Yin, S.H., T.Y. Wung, and K. Chen. 1978. Natural convection in an air layer enclosed within rectangular cavities. *International Journal of Heat and Mass Transfer*, 21: 307-315.

Zhao, Y., W.P. Goss, D. Curcija, J.P. Power. 1997. A new set of analytical correlations for predicting convective heat transfer in fenestration glazing cavities. *CLIMA 2000 Conference in Brussels, Belgium*. September.